Proceedings of the ASME 2012 International Design Engineering Technical Conferences & Computers and Information in Engineering Conference
IDETC/CIE 2012
August 12-15, 2012, Chicago, IL, USA

DETC2012-71119

COMPOSITE MATERIAL TESTING DATA REDUCTION TO ADJUST FOR THE SYSTEMATIC 6-DOF TESTING MACHINE ABERRATIONS

Athanasios Iliopoulos
Computational Materials Science Center
George Mason University, Fairfax VA 22030, USA
resident at Center of Computational Material Science
Naval Research Laboratory
Washington DC 20375, USA

John G. Michopoulos
Computational Multiphysics Systems Lab.
Center of Computational Material Science
Naval Research Laboratory
Washington DC 20375, USA

John C. Hermanson
Wood Based Materials & Structures
Forest Products Laboratory
USDA Forest Service
Madison, WI, USA

ABSTRACT

This paper describes a data reduction methodology for eliminating the systematic aberrations introduced by the unwanted behavior of a multiaxial testing machine, into the massive amounts of experimental data collected from testing of composite material coupons. The machine in reference is a custom made 6-DoF system called NRL66.3 and developed at the NAval Research Laboratory, that consists of multiple sets of hexapod configurations essentially forming a recursive synthesis of multiple parallel mechanisms. Hexapod linkages, the grips, and other deformable parts of the machine absorb energy. This is manifested in an either reversible or irreversible manner, thus introducing a parasitic behavior that is undesirable from the perspective of our ultimate goal of the material constitutive characterization. The data reduction focuses both on the kinematic (pose of the grip) and the reaction (forces and moments) that are critical input quantities of the material characterization process. The kinematic response is reduced by exploitation of the kinematics of the dots used for full field measurements. A correction transformation is identified by solving an inverse problem that minimizes the known displacements at the grips as given by the full field measurements and those given by the machine's displacement sensors. A Procrustes problem formalism was introduced to exploit a known material behavior tested by the testing machine. Consequently, a correction transformation was established and was applied on the load cell data of the machine in order to eliminate the spurious responses appearing in the force and moment data.

INTRODUCTION

During the past decade, the Computational Multiphysics System Laboratory of the Naval Research Lab (NRL) has embarked in an effort to automate massive multiaxial testing of composite coupons in order to determine the constitutive behavior of the bulk composite material used to make these coupons.

The characterization of the constitutive response of composite materials has been traditionally achieved through conventional uniaxial tests and used for determining elastic properties. The identification of these properties, involve uniaxial tests conducted with specimens mounted on testing machines, with the major orthotropic axis of any given specimen inclined relative to

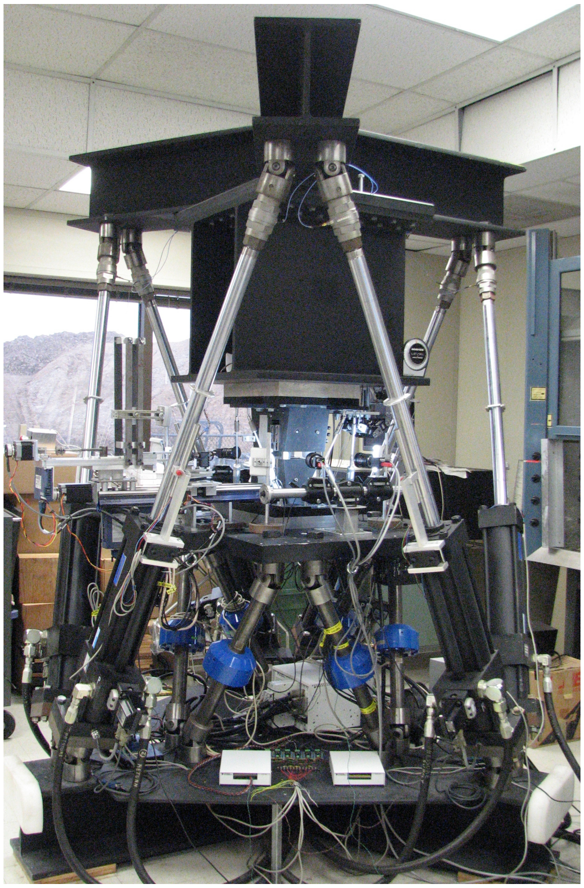

FIGURE 1: THE NRL66.3 6 DoF MECHATRONIC LOADER

the loading direction. Specimens are designed such that a homogeneous state of strain is developed over a well defined area for the purpose of measuring kinematic quantities [1, 2]. Consequently, the use of uniaxial testing machines imposes requirements of using multiple specimens, griping fixtures and multiple experiments. The requirement of a homogeneous state of strain frequently imposes restrictions on the sizes and shapes of specimens to be tested. It follows that these requirements result in increased cost and time, and consequently to inefficient characterization processes.

To address these issues and to extend characterization to non-linear regimes, multi-degree of freedom automated mechatronic testing machines, which are capable of loading specimens multiaxially in conjunction with energy-based inverse characterization methodologies, were introduced at NRL [3–5]. This introduction was the first of its kind and has continued through the present [6–8]. The most recent prototype of these machines, is shown in Fig. 1 and carries the name NRL66.3.

In the context of data-driven inverse characterization, there are two types of data that are expected as output from a loading machine. The first relates to the displacement boundary conditions and the second to the forces and moments imposed on the specimen.

The displacement applied on the specimen measured on the machine actuators, contains both the displacement due to deformation of the specimen and the deformation of the machine itself. Taking advantage of the Mesh-less Random Grid (MRG) method for full - field measurements [9–14], we present a method for the identification of the kinematic quantities imposed only on the specimen.

Although NRL66.3 has recently proven to be very efficient in the inverse characterization of the constitutive response of composite materials [15, 16], the manufacturing aberrations that lead to output data imprecisions has not been studied in detail. Those aberrations are especially important for near-singular configurations, like the one adopted for the design of NRL66.3.

Such configurations raise challenges in the control electronics [17–21] and also result in magnification of reaction forces that can increase the precision of reaction measurement through appropriate load cell configurations. The magnification of reactions is followed by the magnification in the sensitivity on certain loading states that in turn result in the reduction of accuracy on those states. In order to deal with those issues we present a methodology that, based on the known response of a calibration specimen, can be used to identify the linear mapping between the NRL66.3 load cell readings and the expected calibration specimen reaction response.

This paper begins with the description of the problem of identifying the equivalent transformational conditions applied on a boundary, given a set of experimentally measured displacements near the boundary, provides the solution of this problem, and continues with a set of synthetic experiments that show the response of the proposed approach to noisy data. It continues with the formulation and solution of the problem of reducing the reactions, as they are originally collected by the NRL66.3 data acquisition system in raw form, to data that have been corrected for the manufacturing and other aberrations. The paper closes with the presentation of the results of the corrected reaction forces and the associated conclusions.

DISPLACEMENT BOUNDARY CONDITIONS FROM FULL FIELD DATA

In this section we will present a method that can be used to calculate Finite Element (FE) compatible displacement boundary conditions from full field experimental data [9–14, 22].

In mechanics experiments, where the specimen is fixed by pressure grips, the actual boundary conditions are indeterminate. Even if it was possible to adequately identify those boundary conditions, it would still be impractical to incorporate them in the model to be used for material characterization purposes. When the inversion model of the experiment is constructed under an

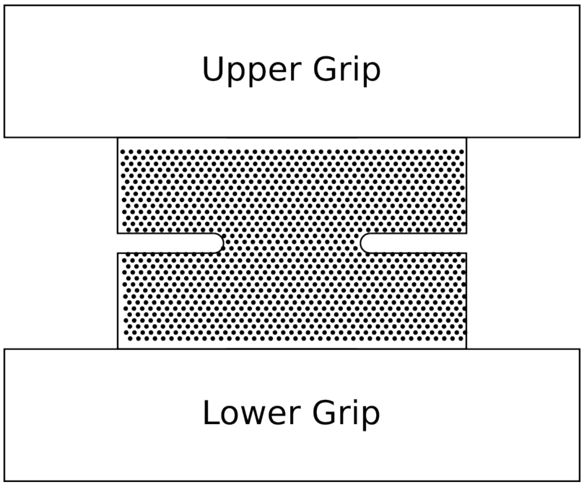

FIGURE 2: SPECIMEN IN THE GRIPS AND FULL FIELD MEASUREMENT DOT PATTERN

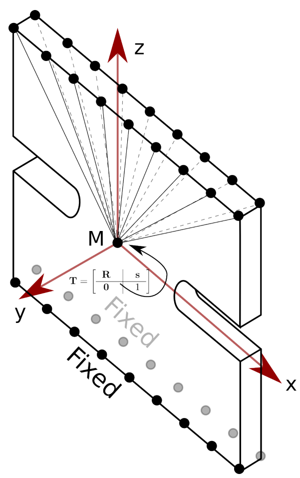

FIGURE 3: BOUNDARY CONDITIONS FOR THE FINITE ELEMENT ANALYSIS

FEM workbench [23, 24], the number of choices becomes even smaller.

A typical specimen used with the Naval Research Laboratory 6-DoF Mechatronic Loader (Fig. 1) for material characterization is shown in Fig. 2. The specimen is gripped on top and bottom and is subjected to any combination of the 6-DoF base kinematic movements (3 displacements and 3 rotations) with the lower grip fixed and the upper grip moving.

When a specimen like this is modeled in a FEA software, the bottom nodes are considered fixed, while the top nodes are considered to be linked to a master node M, that is the instantaneous center of rotation during the test subjected to a 6 DoF motion (Fig. 3). Although this cannot model the actual behavior in detail, it is adequate for the purpose of inverse characterization [23, 24].

NRL66.3 is equipped with two pairs of cameras, that are used to capture the full field of displacements and strain over two opposing surfaces. Such a configuration makes it possible to measure the displacement near the boundaries of the specimen, from both sides and both boundaries. In turn, this allows for a very good approximation of the kinematic behavior of the specimen on the lines the specimen can be considered gripped on.

For the model shown in Fig. 3, we are interested in applying the boundary conditions on nodes that lay on straight lines with the circles, we are seeking the displacement values on those lines. Although not realistic, we are restricted by the FE model in assuming that the boundary lines do retain their linearity during the loading, in order to avoid further complexity in the FE model formulation.

The kinematic boundary conditions of the master node M, are depicted in Fig. 4. The specimen at rest is shown in Fig. 4(a). When it is deformed, both the lower and upper lines at the intersection with the grips will transform at new positions as shown in Fig. 4(b). Since we consider that the shape of those lines doesn't change, their movement can be considered a rigid transformation,

$$\mathbf{T}_1 = \left[\begin{array}{c|c} \mathbf{R}_1 & \mathbf{s}_1 \\ \hline \mathbf{0} & 1 \end{array}\right], \mathbf{T}_2 = \left[\begin{array}{c|c} \mathbf{R}_2 & \mathbf{s}_2 \\ \hline \mathbf{0} & 1 \end{array}\right], \tag{1}$$

where T_1, T_2 are the transformation matrices of the lower and upper faces respectively, R_1, R_2 are the rotation matrices of the lower and upper faces respectively and $\mathbf{s}_1, \mathbf{s}_2$ are the translation of the lower and upper faces respectively (Fig. 4(c)).

In order to identify equivalent boundary conditions like those that are imposed on the FE model (Fig. 3), we need to transform both the lower and upper faces so that the lower face at the deformed configuration coincides with the undeformed boundary. This can be simply done by multiplying both transformations by the inverse of $\mathbf{T}_1$. In such a case the lower face transformation will be the identity (i.e. the face doesn't move) and the upper part will take the desired value (Fig. 4(d)):

$$\left.\begin{array}{l} \mathbf{T}'_1 = \mathbf{T}_1\mathbf{T}_1^{-1} = \left[\begin{array}{c|c} \mathbf{I} & \mathbf{0} \\ \hline \mathbf{0} & 1 \end{array}\right] \\ \mathbf{T}_M = \mathbf{T}'_2 = \mathbf{T}_2\mathbf{T}_1^{-1} \end{array}\right\}. \tag{2}$$

The problem has now been reduced to the identification of the transformation matrices from sets of points that are measured experimentally through the employed full-field method. Formally the problem can be set as follows:

Problem 1. *Given a set of N points* $\mathbf{x}_i = \{x_i, y_i, z_i\}^T, i = 1 \ldots N$ *at an initial configuration and the same set of points at a rigidly*

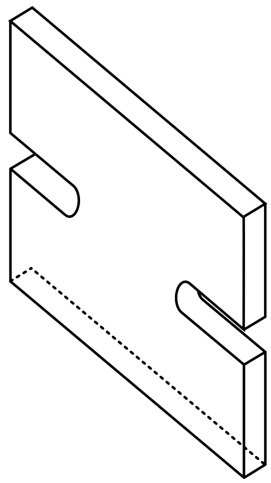

(a) Undeformed specimen

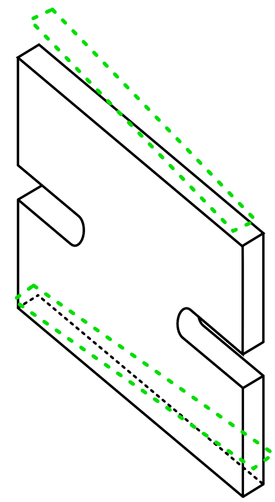

(b) Undeformed specimen and deformed (Dashed Green) lower and upper faces

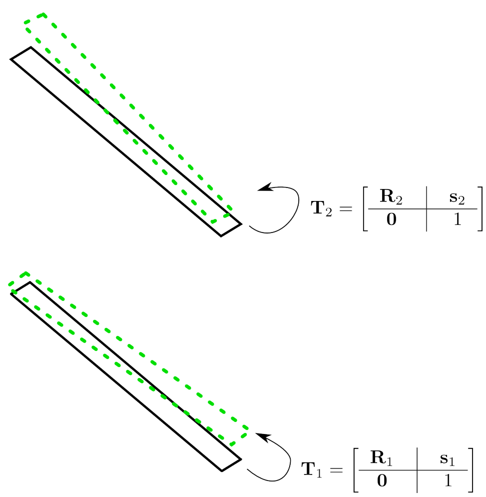

(c) Undeformed, deformed (Dashed Green) faces, and transformation matrices

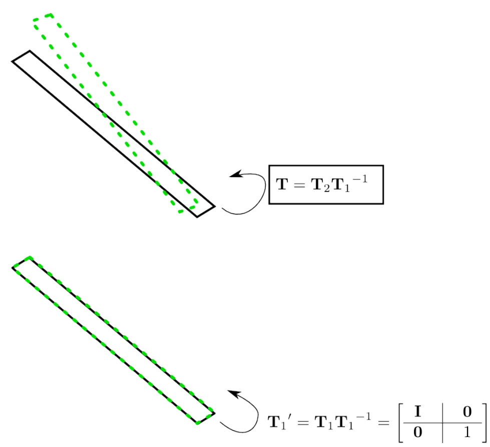

(d) Adjustement relative to the lower faces

FIGURE 4: BOUNDARY TRANSFORMATIONS

transformed configuration $\mathbf{x}'_i = \{x'_i, y'_i, z'_i\}^T, i = 1 \ldots N$, *find a transformation* $\mathbf{T} = \left[\begin{array}{c|c} \mathbf{R} & \mathbf{s} \\ \hline \mathbf{0} & 1 \end{array}\right]$, *with* $\mathbf{R}$ *an orthogonal matrix and* $\mathbf{s}$ *a translation vector, such as* $\sum_i \left(\mathbf{x}_i^h - \mathbf{T}\mathbf{x_i}'^h\right)^2$ *is minimum with* $\mathbf{x}_i^h$ *and* $\mathbf{x}_i'^h$ *the homogenous representation of vectors* $\mathbf{x}_i$ *and* $\mathbf{x}'_i$.

Although this problem can be at first considered an iterative optimization problem, it has a more elegant algebraic solution that can be achieved by using the properties of solution to the orthogonal Procrustes problem [25–27].

We translate both vector sets so that their mean is at the origin, in order to consider only the rotational part of the transformation,

$$\left.\begin{aligned} \mathbf{w}_i &= \{r_i, s_i, t_i\}^T = \mathbf{x}_i - \mathbf{t} \\ \mathbf{w}'_i &= \left\{r'_i, s'_i, t'_i\right\}^T = \mathbf{x}'_i - \mathbf{t}' \end{aligned}\right\}, \tag{3}$$

where $t = \frac{1}{N}\sum_{i=1}^N x_i$ and $t' = \frac{1}{N}\sum_{i=1}^N x'_i$

From those vectors we form the following matrices,

$$\mathbf{W} = \{\mathbf{w}_1, \mathbf{w}_2, \ldots, \mathbf{w}_N\} = \begin{bmatrix} r_1 & r_2 & \ldots & r_N \\ s_1 & s_2 & \ldots & s_N \\ t_1 & t_2 & \ldots & t_N \end{bmatrix} \tag{4}$$

and

$$\mathbf{W}' = \{\mathbf{w}'_1, \mathbf{w}'_2, \ldots, \mathbf{w}'_N\} = \begin{bmatrix} r'_1 & r'_2 & \ldots & r'_N \\ s'_1 & s'_2 & \ldots & s'_N \\ t'_1 & t'_2 & \ldots & t'_N \end{bmatrix} \tag{5}$$

and calculate the product:

$$\mathbf{A} = \mathbf{W}'\mathbf{W}^T. \tag{6}$$

We can decompose $\mathbf{A}$ using the Singular Value Decomposition (SVD) in the product of three matrices:

$$\mathbf{A} = \mathbf{USV}^T. \tag{7}$$

According to [27] the orthogonal matrix that transforms $\mathbf{w_i}$s to $\mathbf{w'_i}$s is given by,

$$\mathbf{R} = \mathbf{UZV}^T, \tag{8}$$

with:

$$\mathbf{Z} = \begin{bmatrix} 1 & 0 & 0 \\ 0 & 1 & 0 \\ 0 & 0 & \det(\mathbf{UV}^T) \end{bmatrix}, \tag{9}$$

a matrix that is used to handle cases with the determinant of $\mathbf{R}$ being negative. Writing all the transformations in a compact form results in the global transformation matrix that transforms $\mathbf{x_i^h}$s to $\mathbf{x_i'^h}$s:

$$\mathbf{T} = \left[\begin{array}{c|c} \mathbf{I} & \mathbf{t}' \\ \hline \mathbf{0} & 1 \end{array}\right] \left[\begin{array}{c|c} \mathbf{R} & \mathbf{0} \\ \hline \mathbf{0} & 1 \end{array}\right] \left[\begin{array}{c|c} \mathbf{I} & -\mathbf{t} \\ \hline \mathbf{0} & 1 \end{array}\right] = \left[\begin{array}{c|c} \mathbf{R} & \mathbf{t}' - \mathbf{Rt} \\ \hline \mathbf{0} & 1 \end{array}\right]. \tag{10}$$

Eq. (10) is used to find both the transformations of Eq. (1) that are then used in Eq. (2) to calculate the transformation of the master node M.

In order to evaluate the effectiveness of the proposed algorithm we performed a number of synthetic experiments. A set of 150 random points was generated and then translated on 3 axes by $\mathbf{s}$ and rotated on 3 axes by $\mathbf{R}(\theta, \phi, \omega)$ as shown in Fig. 5. The transformed points where perturbed using a random number generator to simulate different noise levels. The noise levels varied from 0% to 10% of the maximum point distance. For each noisy set, the methodology presented was applied and the transformation matrix $\mathbf{T}$ was identified. Then a simple iterative algorithm was employed [28, 29] to identify the values of the angles on the identified rotation matrix. The mean absolute error on the angle results of the synthetic experiments is shown in Fig. 6.

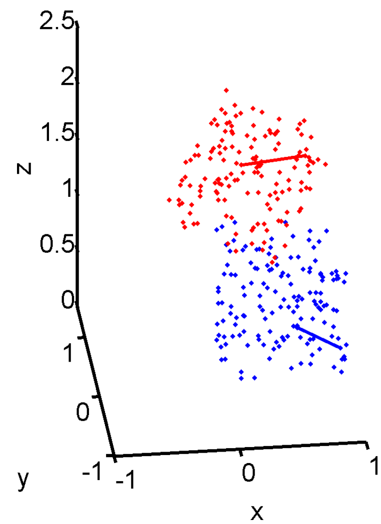

FIGURE 5: RANDOM POINTS (BLUE) AND THEIR RIGID BODY TRANSFORMATION (RED)

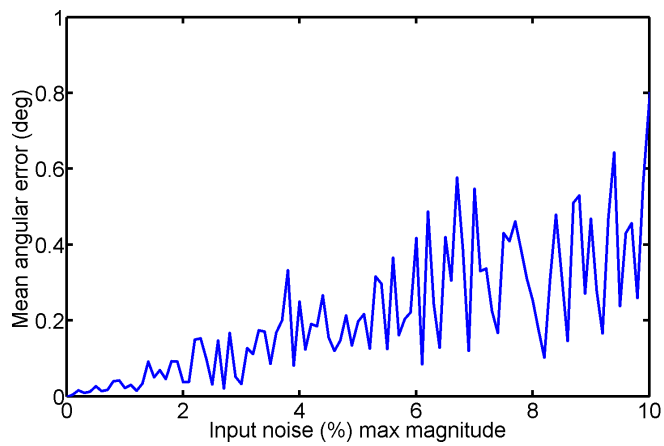

FIGURE 6: MEAN ABSOLUTE ANGLE IDENTIFICATION ERROR VS NOISE LEVEL

REDUCTION OF REACTIONS

NRL66.3 reaction measurements

To achieve measurement of the reaction forces and moments, NRL66.3 is equipped with a set of 6 load cells in the legs that form the lower hexapod (Fig. 1). A sketch of the hexapod configuration is shown in Fig. 7.

Each of the 6 legs of the hexapod, is defined between two end points B_i and B'_i, , $i = 1 \ldots 6$ that can be represented by the vectors $\mathbf{b}_i = \{x_i, y_i, z_i\}^T$ and $\mathbf{b}'_i = \{x'_i, y'_i, z'_i\}^T$ respectively relative to the base coordinate system $Oxyz$. The reaction forces measured on the legs of the hexapod are to be used to calculate the forces and moments applied on the specimen. We consider that the coordinate system $O^s x^s y^s z^s$ (that the forces and moments are

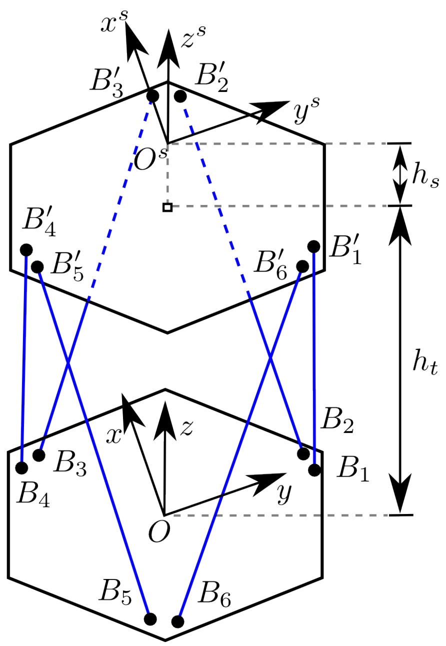

FIGURE 7: REACTION MEASUREMENT HEXAPOD CONFIGURATION

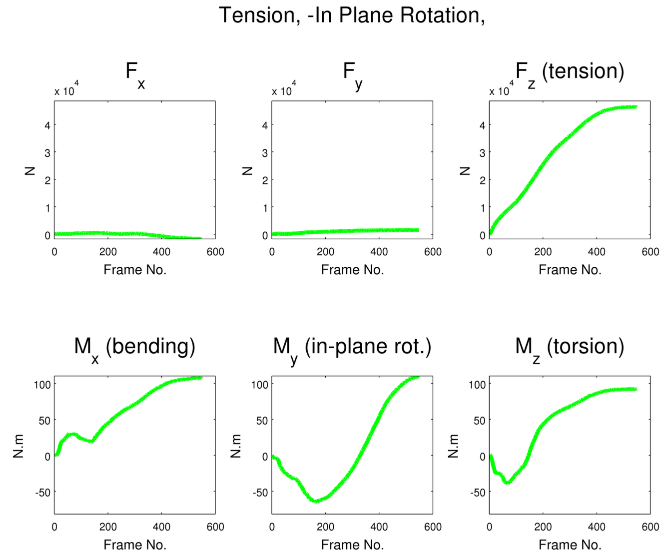

FIGURE 8: REACTION FORCES AND MOMENTS OF A TENSION,IN PLANE ROTATION EXPERIMENT AS CALCULATED BY EQ. (14)

to be transformed to), is at the center of the specimen (as also assumed in Fig. 3), that is located vertically from the base coordinate system at a distance $h = h_t + h_s$.

If the magnitude of force measured on each load cell is equal to $f_i, i = 1 \dots 6$, then the total force vector can be easily calculated by,

$$\mathbf{f} = \sum_{i=1}^{6} \mathbf{n}_i f_i = \begin{bmatrix} n_1^x \ n_2^x \dots n_6^x \\ n_1^y \ n_2^y \dots n_6^y \\ n_1^z \ n_2^z \dots n_6^z \end{bmatrix} \begin{bmatrix} f_1 \\ f_2 \\ f_3 \\ f_4 \\ f_5 \\ f_6 \end{bmatrix}, \tag{11}$$

where $\mathbf{n}_i = \left\{ n_i^x, n_i^y, n_i^z \right\}^T = \frac{\mathbf{b}'_i - \mathbf{b}_i}{|\mathbf{b}'_i - \mathbf{b}_i|}$ is the unit vector between B_i and B'_i. The moments vector applied around O^s can be calculated by [17],

$$\mathbf{m} = \sum_{i=1}^{6} [\mathbf{r}_i \times \mathbf{n}_i] f_i, \tag{12}$$

where $\mathbf{r}_i$ is the vector that defines the position of the base end points B_i relative to the $O^s x^s y^s z^s$ coordinate system and is given by:

$$\mathbf{r}_i = \{x_i, y_i, z_i - h\}^T. \tag{13}$$

The equations (11) and (12) can be written in compact form as,

$$\mathbf{a} = \left[\frac{\mathbf{f}}{\mathbf{m}}\right] = \begin{bmatrix} f_x \\ f_y \\ f_z \\ \hline m_x \\ m_y \\ m_z \end{bmatrix} = \\ = \mathbf{H} \begin{bmatrix} f_1 \\ f_2 \\ f_3 \\ f_4 \\ f_5 \\ f_6 \end{bmatrix} = \left[\begin{array}{cccc} \mathbf{n}_1 & \mathbf{n}_2 & \dots & \mathbf{n}_6 \\ \hline \mathbf{r}_1 \times \mathbf{n}_1 & \mathbf{r}_2 \times \mathbf{n}_2 & \dots & \mathbf{r}_6 \times \mathbf{n}_6 \end{array} \right] \begin{bmatrix} f_1 \\ f_2 \\ f_3 \\ f_4 \\ f_5 \\ f_6 \end{bmatrix}, \tag{14}$$

where $\mathbf{H}$ is the 6×6 characteristic matrix of the reactions calculation equation.

Although Eq. (14) is relatively straightforward, it suffers from a serious weakness; it does not account for the manufacturing aberrations of the measurement system. The measurement sensitivity relative to those aberrations is even more important in the case of NRL66.3, which is designed in a near singular configuration. Such a configuration achieves high magnification of forces and moments (and hence higher precision) [21] but because of the higher sensitivity of such a configuration, results in parasitic effects due to manufacturing tolerances.

Reduction methodology

To show the difference the machine aberrations make in the results we present in Fig. 8, the resulting moments and forces of a tension, in-plane rotation experiment. In this case we wouldn't expect any bending (M_x) and torsion (M_z) moments, but the raw data falsely indicate so.

To resolve this issue we could either implement a constructive tolerance analysis that would involve a large number of parameters and result in large non-linear expressions or correct for the aberrations by employing an inversion procedure. The latest approach is more appealing, because not only it would reduce for known systematic tolerances, but can potentially reduce for unknown systematic and random aberrations. Similar methodologies have been developed by others in various contexts [30–33].

Employing such a procedure means that we should develop a methodology to inversely identify the characteristic matrix of the reaction calculation, based on data from well known responses to various loading paths. Those responses can then be used in yet another inversion problem to create a linear (but potentially nonlinear) mapping between the NRL66.3 load cell values and the expected reaction forces.

Such a methodology should involve the following steps:

1. Execute a set of experiments with a geometry and a material of a well known response relative to various loading paths and measure the strain tensor components on the surface of the specimens via a Full-Field technique.
2. Using the response from the Full-Field technique inversely identify the boundary conditions.
3. For the chosen set of experiments identify the mapping between the machine load cell readings and the boundary conditions of step 2.

A flat plate from a linearly elastic material like aluminum or steel can provide an adequate specimen for the purpose of inverse identification of the reaction response. The continuum model to be used for inversion can be either constructed analytically or numerically through any FE software. For this work we chose to use the FE approach.

In order to identify the boundary conditions we are seeking to define an optimization problem with the FE model boundary forces as design variables and an objective function based on a norm of the surface strain. A least square objective function that satisfies those requirements can be defined as,

$$\min_{\mathbf{a}\in\mathbb{R}^6} \sum_{j=1}^{M} \left[\left({}^{e}\varepsilon_{xx}^{j} - {}^{f}\varepsilon_{xx}^{f}\right)^2 + \left({}^{e}\varepsilon_{yy}^{j} - {}^{f}\varepsilon_{yy}^{j}\right)^2 + \left({}^{e}\varepsilon_{xy}^{j} - {}^{f}\varepsilon_{xy}^{j}\right)^2 \right], \tag{15}$$

where M is the number of evaluation points, ${}^{e}\varepsilon_{xx}^{j}, {}^{e}\varepsilon_{yy}^{j}, {}^{e}\varepsilon_{xy}^{j}$ are the values of the strain components at the j evaluation point from the Full-Field measurement, ${}^{f}\varepsilon_{xx}^{j}, {}^{f}\varepsilon_{yy}^{j}, {}^{f}\varepsilon_{xy}^{j}$ are the values of the strain components at the j evaluation point calculated from the FE analysis and $\mathbf{a} = \left\{\mathbf{f}^T, \mathbf{m}^T\right\}^T = \left\{f_x, f_y, f_z, m_x, m_y, m_z\right\}^T$ is the vector that collects the reaction forces and moments. It should be noted that the values of strain from the finite element analysis (${}^{f}\varepsilon_{xx}^{j}, {}^{f}\varepsilon_{yy}^{j}, {}^{f}\varepsilon_{xy}^{j}$) are functions of the vector $\mathbf{a}$.

Although it is possible to use an iterative solver to solve the minimization problem of Eq. 15 it would be much more efficient to develop an algebraic formulation.

Towards that end we notice that since we are interested in the FE solution in the linear elastic regime, we are allowed to use the superposition principle to combine two or more solutions. For example if the ε_{xx} strain result of the FE analysis for unit tensile loading ($\mathbf{a} = \{0,0,1,0,0,0\}^T$) for a node j is ${}^{f}\varepsilon_{xx}^{j}(0,0,1,0,0,0)$ and for the same node the ε_{xx} strain result of the FE analysis for unit torsion loading ($\mathbf{a} = \{0,0,0,0,0,1\}^T$) is ${}^{f}\varepsilon_{xx}^{j}(0,0,1,0,0,0)$, then the combined tension-torsion analysis would result in:

$${}^{f}\varepsilon_{xx}^{j}(0,0,1,0,0,1) = {}^{f}\varepsilon_{xx}^{j}(0,0,1,0,0,0) + {}^{f}\varepsilon_{xx}^{j}(0,0,0,0,0,1) \tag{16}$$

Building on this observation, we can construct a semi-analytic process of calculating the strain on every node j of the FE analysis as follows,

$$\begin{aligned}
&{}^{f}\varepsilon_{xx}^{j}(f_x, f_y, f_z, m_x, m_y, m_z) = \\
&= f_x {}^{f}\varepsilon_{xx}^{j}(1,0,0,0,0,0) + \\
&+ f_y {}^{f}\varepsilon_{xx}^{j}(0,1,0,0,0,0) + \\
&+ f_z {}^{f}\varepsilon_{xx}^{j}(0,0,1,0,0,0) + \\
&+ m_x {}^{f}\varepsilon_{xx}^{j}(0,0,0,1,0,0) + \\
&+ m_y {}^{f}\varepsilon_{xx}^{j}(0,0,0,0,1,0) + \\
&+ m_z {}^{f}\varepsilon_{xx}^{j}(0,0,0,0,0,1) = \\
&= {}_{1}^{f}\varepsilon_{xx}^{j} f_x + {}_{2}^{f}\varepsilon_{xx}^{j} f_y + {}_{3}^{f}\varepsilon_{xx}^{j} f_z + {}_{4}^{f}\varepsilon_{xx}^{j} m_x + {}_{5}^{f}\varepsilon_{xx}^{j} m_y + {}_{6}^{f}\varepsilon_{xx}^{j} m_z,
\end{aligned} \tag{17}$$

where:

$$\left.\begin{aligned}
{}_{1}^{f}\varepsilon_{xx}^{j} &= {}^{f}\varepsilon_{xx}^{j}(1,0,0,0,0,0) \\
{}_{2}^{f}\varepsilon_{xx}^{j} &= {}^{f}\varepsilon_{xx}^{j}(0,1,0,0,0,0) \\
{}_{3}^{f}\varepsilon_{xx}^{j} &= {}^{f}\varepsilon_{xx}^{j}(0,0,1,0,0,0) \\
{}_{4}^{f}\varepsilon_{xx}^{j} &= {}^{f}\varepsilon_{xx}^{j}(0,0,0,1,0,0) \\
{}_{5}^{f}\varepsilon_{xx}^{j} &= {}^{f}\varepsilon_{xx}^{j}(0,0,0,0,1,0) \\
{}_{6}^{f}\varepsilon_{xx}^{j} &= {}^{f}\varepsilon_{xx}^{j}(0,0,0,0,0,1)
\end{aligned}\right\}. \tag{18}$$

Rewriting Eq. (17) in vector form yields,

$${}^{f}\varepsilon_{xx}^{j}(f_x, f_y, f_z, m_x, m_y, m_z) = {}^{f}\varepsilon_{xx}^{j}(\mathbf{a}) = \boldsymbol{\varepsilon}_{xx}^{jT}\mathbf{a}. \tag{19}$$

where $\boldsymbol{\varepsilon}_{xx}^{jT} = \left\{ {}^f_1\varepsilon_{xx}^j, {}^f_2\varepsilon_{xx}^j, {}^f_3\varepsilon_{xx}^j, {}^f_4\varepsilon_{xx}^j, {}^f_5\varepsilon_{xx}^j, {}^f_6\varepsilon_{xx}^j \right\}$ is the vector that collects the ε_{xx} strain component of node j of each of the 6 base cases of Eq. (18). There are two major benefits using this semi-analytic (or semi-numerical) approach: (a) We can calculate the strain fields without the need to run a finite element analysis for any load combination and (b) It can be used to construct complex linear systems of interest.

For each node j we can collect the stain components such as we can form a vector of the form,

$$\boldsymbol{\varepsilon}_f^j = \mathbf{E}^j \mathbf{a}, \tag{20}$$

where $\boldsymbol{\varepsilon}_f^j = \left\{ {}^f\varepsilon_{xx}^j(\mathbf{a}), {}^f\varepsilon_{yy}^j(\mathbf{a}), {}^f\varepsilon_{xy}^j(\mathbf{a}) \right\}^T$ and

$$\mathbf{E}^j = \begin{bmatrix} \boldsymbol{\varepsilon}_{xx}^{jT} \\ \boldsymbol{\varepsilon}_{yy}^{jT} \\ \boldsymbol{\varepsilon}_{xy}^{jT} \end{bmatrix}. \tag{21}$$

If we furthermore collect the vectors $\boldsymbol{\varepsilon}_f^j$ for all M nodes we can form a vector of the form:

$$\mathbf{e}_f = \begin{bmatrix} \boldsymbol{\varepsilon}_f^1 \\ \boldsymbol{\varepsilon}_f^2 \\ \vdots \\ \boldsymbol{\varepsilon}_f^M \end{bmatrix} = \begin{bmatrix} \mathbf{E}^1 \\ \mathbf{E}^2 \\ \vdots \\ \mathbf{E}^M \end{bmatrix} \mathbf{a} = \mathbf{E}\mathbf{a}. \tag{22}$$

Similarly, collecting the strain components from the Full-Field measurements such as,

$$\boldsymbol{\varepsilon}_e = \begin{bmatrix} {}^e\varepsilon_{xx}^1 \\ {}^e\varepsilon_{yy}^1 \\ {}^e\varepsilon_{xy}^1 \\ {}^e\varepsilon_{xx}^2 \\ {}^e\varepsilon_{yy}^2 \\ {}^e\varepsilon_{xy}^2 \\ \vdots \\ {}^e\varepsilon_{xx}^M \\ {}^e\varepsilon_{yy}^M \\ {}^e\varepsilon_{xy}^M \end{bmatrix}, \tag{23}$$

we can form a system of equations of the form:

$$\mathbf{E}\mathbf{a} = \boldsymbol{\varepsilon}_e. \tag{24}$$

The system of Eq. 24 is an overdetermined system of $3 \times M$ equations. We can seek an $\mathbf{a}$, such as $\|\mathbf{E}\mathbf{a} - \boldsymbol{\varepsilon}_e\|$ is minimized, where $\|\circ\|$ is the vector norm. Such a $\mathbf{a}$ is known as the least squares solution to the over-determined system. Closer observation reveals that the vector norm is actually the objective function we seek to minimize in Eq. (15) . A solution can be given by the following equation,

$$\mathbf{a} = \mathbf{V}\mathbf{y}, \tag{25}$$

where $\mathbf{V}$ is calculated by the Singular Value Decomposition (SVD) of $\mathbf{E}$ as,

$$\mathbf{U}\mathbf{D}\mathbf{V}^T = \mathbf{E}, \tag{26}$$

where $\mathbf{y}$ is a vector defined as $y_i = b_i{}'/d_i$, $\mathbf{b} = b_i$ is a vector given by,

$$\mathbf{b} = \mathbf{U}^T\mathbf{a} \tag{27}$$

and d_i is the ith entry of the diagonal of $\mathbf{D}$.

The solution of the inverse problem as described by the overdetermined system of Eq. (24) gives the reaction vector $\mathbf{a}$ that if applied to the FE model of the calibration specimen will result in surface strains that approximate the ones from the Full-Field measurement in a least squares manner. In other words this solution gives the force boundary conditions of the model, that best approximates a certain surface strain state.

The last problem that remains to be solved is that of mapping the results of the calibration of a set of loading conditions to the reaction vector calculated by the the solution of systems like those in Eq. (24). From a single calibration experiment we will have a number of reaction vector pairs $\mathbf{a}_k \leftrightarrow \mathbf{c}_k$ for each loading step $k = 1 \ldots K$ and for L experiments of various loading paths we will have a total of $L \times K$ pairs,

$$\mathbf{a}_l \leftrightarrow \mathbf{c}_l, l = 1 \ldots L \times K, \tag{28}$$

where $\mathbf{c}_l = \{f_1, f_2, f_3, f_4, f_5, f_6\}^T$ is the vector of the forces measured on the base load cells. Based on Eq. (14) we want to identify a linear transformation $\mathbf{H}$ such as:

$$\mathbf{a}_l = \mathbf{H}\mathbf{c}_l. \tag{29}$$

The previous equation can be rewritten in a single linear sys-

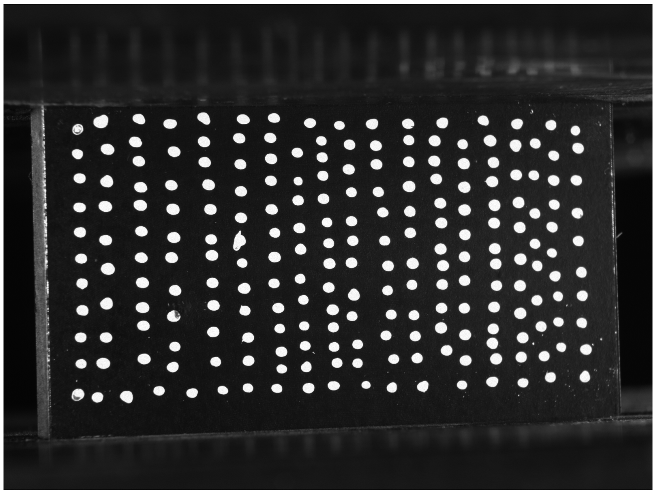

FIGURE 9: FLAT ALUMINUM SPECIMEN IN THE GRIPS

tem as,

$$\begin{bmatrix} \mathbf{c}_1^T & \mathbf{0}_6 & \mathbf{0}_6 & \mathbf{0}_6 & \mathbf{0}_6 & \mathbf{0}_6 \\ \mathbf{0}_6 & \mathbf{c}_1^T & \mathbf{0}_6 & \mathbf{0}_6 & \mathbf{0}_6 & \mathbf{0}_6 \\ \mathbf{0}_6 & \mathbf{0}_6 & \mathbf{c}_1^T & \mathbf{0}_6 & \mathbf{0}_6 & \mathbf{0}_6 \\ \mathbf{0}_6 & \mathbf{0}_6 & \mathbf{0}_6 & \mathbf{c}_1^T & \mathbf{0}_6 & \mathbf{0}_6 \\ \mathbf{0}_6 & \mathbf{0}_6 & \mathbf{0}_6 & \mathbf{0}_6 & \mathbf{c}_1^T & \mathbf{0}_6 \\ \mathbf{0}_6 & \mathbf{0}_6 & \mathbf{0}_6 & \mathbf{0}_6 & \mathbf{0}_6 & \mathbf{c}_1^T \\ \vdots & \vdots & \vdots & \vdots & \vdots & \vdots \\ \mathbf{0}_6 & \mathbf{0}_6 & \mathbf{0}_6 & \mathbf{0}_6 & \mathbf{0}_6 & \mathbf{c}_{L\times K}^T \end{bmatrix} \begin{bmatrix} \mathbf{h}_1^T \\ \mathbf{h}_2^T \\ \mathbf{h}_3^T \\ \mathbf{h}_4^T \\ \mathbf{h}_5^T \\ \mathbf{h}_6^T \end{bmatrix} = \begin{bmatrix} \mathbf{a}_1^T \\ \vdots \\ \mathbf{a}_{L\times M}^T \end{bmatrix} \qquad (30)$$

or

$$\mathbf{C}\mathbf{h}_v = \mathbf{a}_v, \qquad (31)$$

where $\mathbf{h}_p$ is the pth row of $\mathbf{H}$, $\mathbf{h}_v = \{\mathbf{h}_1, \mathbf{h}_1, \mathbf{h}_2, \mathbf{h}_3, \mathbf{h}_4, \mathbf{h}_5, \mathbf{h}_6\}^T$, $\mathbf{a}_v = \{\mathbf{a}_1, \ldots, \mathbf{a}_{L\times M}\}^T$ and $\mathbf{0}_6 = \{0,0,0,0,0,0\}$. Using a similar approach we followed in the system of Eq. (24) we can obtain the value of the components of $\mathbf{h}_v$ (and consequently of $\mathbf{H}$ that minimize the vector norm $\|\mathbf{C}\mathbf{h}_v - \mathbf{a}_v\|$). This solution is the least squares solution to the system of Eqs. 31.

Application of the reaction reduction

The calibration specimen used was manufactured out of Al-5083 alloy with the properties shown in Table 1. The calibration specimen was then marked with a pattern of black dots as shown in Fig. 9 so that the full field of strain could be identified by employing the Mesh-Less Random Grid Method (MRG) [9–14, 34]. The experiments included multiple repetitions of all the base cases: (a) displacement on the x axis, (b) displacement on the y axis, (c) displacement on the z axis, (d) rotation around the x axis, (e) rotation around the y axis and (f) rotation around the z axis.

TABLE 1: AL-5083 MECHANICAL PROPERTIES

Parameter	Value	Units
E	72.0×10^9	N/m^2
ν	0.33	

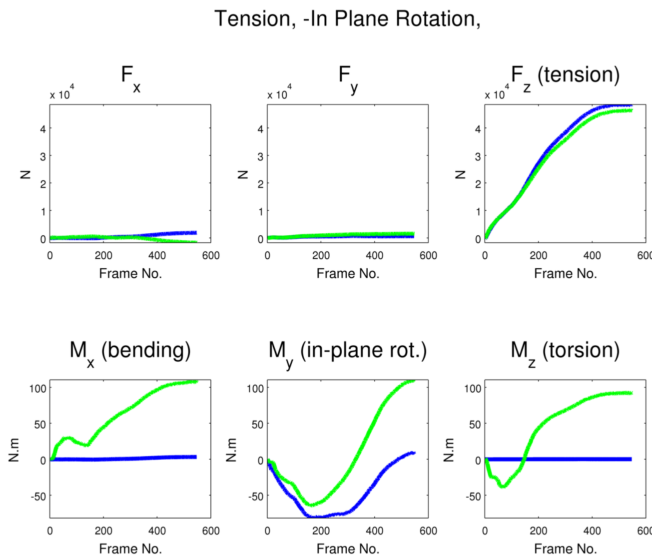

FIGURE 10: REACTION FORCES AND MOMENTS OF A TENSION,IN PLANE ROTATION EXPERIMENT AS CALCULATED BY EQ. (14) (GREEN) AND AS CALCULATED BY THE REDUCTION METHODOLOGY (BLUE).

The calibration experiments resulted in sets of full field strains, that were evaluated at the FE model nodes to form the system of Eqs. (24). The solution of this system for all load steps and all loading cases was then used to form the linear system of Eq. (31). The least squares solution of the last system gives the 6×6 characteristic matrix of the reactions calculation equation.

Using Eq. (14) for each load step of every experiment yields the reduced force-moment vectors $\mathbf{a}$ that are corrected for manufacturing aberrations. The corrected forces and moments for the case presented earlier are shown in blue in Fig. 10. It is evident from this figure that as expected the forces on x, y axes as well as the moments around x and z axes are close to zero, while the tensile force (z axis) and the in-plane rotation moment (y axis), behave as expected.

The same procedure was used to reduce the forces of the experiments conducted at NRL and resulted in new set of data that are free from the aberrations of the robotic loader.

CONCLUSIONS

In this paper the reduction of the NRL66.3 6-DoF robotic loader experimental data output was presented. Specifically, the reduction of the two types of boundary conditions (displacement b.c.s and reaction b.c.s) was derived.

The displacement boundary conditions were represented in a transformational form of 3 translations and 3 rotations on a master node. Their calculation was done with the aid of the full field measurement subsystem of the NRL66.3 [35, 36] and its solution was carried out by transforming the problem to a Procrustes equivalent problem that can be solved algebraically.

The reaction boundary conditions were calculated with the aid of a calibration specimen of know mechanical properties. The reactions forces and moment of this specimen relative to its kinematic response (measured with the MRG method) were identified by an algebraic inversion procedure of the continuum problem represented as the results of base Finite Element Analyses. The linear transformation that maps the NRL66.3 load cell data to the identified reaction forces and moments was calculated by solving yet another inversion problem through its algebraic representation. The resulting transformation was used to correct the reaction output of NRL66.3.

ACKNOWLEDGMENT

The authors acknowledge support for this work by the Office of Naval Research and the Naval Research Laboratory's core funding.

REFERENCES

[1] Daniel, I. M., and Ishai, O., 2005. *Engineering Mechanics of Composite Materials*, 2nd ed. Oxford University Press, USA, July.

[2] Carlsson, L., Adams, D. F., and Pipes, R. B., 1986. *Experimental Characterization of Advanced Composite Materials, Third Edition*, 3 ed. CRC Press, Dec.

[3] Mast, P., Beaubien, L., Clifford, M., Mulville, D., Sutton, S., Thomas, R., Tirosh, J., and Wolock, I., 1983. "A semi-automated in-plane loader for materials testing". *Experimental Mechanics,* ***23***, pp. 236–241. 10.1007/BF02320415.

[4] Mast, P. W., Nash, G. E., Michopoulos, J. G., Thomas, R. W., Badaliance, R., and Wolock, I., 1992. Experimental determination of dissipated energy density as a measure of strain-induced damage in composites. Tech. Rep. Tec. Rpt. NRL/FR/6383–92-9369, Naval Research Laboratory, Washington, DC, USA.

[5] Mast, P., Nash, G., Michopoulos, J., Thomas, R., Wolock, I., and Badaliance, R., 1995. "Characterization of strain-induced damage in composites based on the dissipated energy density Part I. Basic scheme and formulation". *Theoretical and Applied Fracture Mechanics,* ***22***(2), pp. 71–96.

[6] Michopoulos, J., 2003. *Recent advances in Composite Materials: In Honor Of S.A. Paipetis*. Kluwer Academic Press, ch. Computational and Mechatronic Automation of Multiphysics Research for Structural and Material Systems, pp. 9–21.

[7] Michopoulos, J., 2004. "Mechatronically automated characterization of material constitutive respone". In Proceedings of the 6th World Congress on Computational Mechanics (WCCM-VI), Tsinghua University Press and Springer, pp. 486–491.

[8] Michopoulos, J., Hermanson, J., and Furukawa, T., 2008. "Towards the robotic characterization of the constitutive response of composite materials". *Composite Structures,* ***86***(1-3), pp. 154–164.

[9] Michopoulos, J. G., Iliopoulos, A. P., and Furukawa, T., 2009. "Accuracy of inverse composite laminate characterization via the mesh free random grid method". *ASME Conference Proceedings,* ***2009***(48999), pp. 367–374.

[10] Andrianopoulos, N. P., and Iliopoulos, A. P., 2006. "Displacements measurement in irregularly bounded plates using mesh free methods". In Proc. 16th European Conference of Fracture, Alexandroupolis, Greece, July 3–7.

[11] Iliopoulos, A. P., Michopoulos, J. G., and Andrianopoulos, N. P., 2008. "Performance sensitivity analysis of the Mesh-Free Random Grid method for whole field strain measurements". *ASME Conference Proceedings,* ***2008***(43277), pp. 545–555.

[12] Iliopoulos, A. P., Michopoulos, J. G., and Andrianopoulos, N. P., 2010. "Performance analysis of the Mesh-Free Random Grid Method for full-field synthetic strain measurements". *Strain*, p. In Print.

[13] Iliopoulos, A., and Michopoulos, J., 27–31 Jul 2009. "Sensitivity analysis of the mesh-free random grid method for measuring deformation fields on composites". In Proceedings of the 17th International Conference on Composite Materials, ICCM-17, Edinburgh, The British Composites Society: Edinburgh International Convention Centre (EICC), Edinburgh, UK, 2009.

[14] Iliopoulos, A. P., and Michopoulos, J. G., 2009. "Effects of anisotropy on the performance sensitivity of the Mesh-Free random grid method for whole field strain measurement". *ASME Conference Proceedings,* ***2009***(48999), Jan., pp. 65–74.

[15] Michopoulos, J., Hermanson, J. C., and Iliopoulos, A., 2012. "First industrial strength multi-axial robotic test-

ing campaign for composite material characterization". In Proceedings of the ASME 2012 International Design Engineering Technical Conferences & Computers and Information in Engineering Conference IDETC/CIE, August 12-15, 2012, Chicago, IL, USA. Submitted.

[16] Michopoulos, J.and Iliopoulos, A., and Hermanson, J. C., 2012. "Preliminary validation of composite material constitutive characterization". In Proceedings of the ASME 2012 International Design Engineering Technical Conferences & Computers and Information in Engineering Conference IDETC/CIE, August 12-15, 2012, Chicago, IL, USA. Submitted.

[17] Ma, O., and Angeles, J., 1991. "Architecture singularities of platform manipulators". In Robotics and Automation, 1991. Proceedings., 1991 IEEE International Conference on, pp. 1542 –1547 vol.2.

[18] Hou, Y., Yao, J., Lu, L., and Zhao, Y., 2006. "Calibration of a pre-stressed stewart platform-based forcre/torque sensor". In Mechatronics and Automation, Proceedings of the 2006 IEEE International Conference on, pp. 2324 –2329.

[19] Ranganath, R., Nair, P., Mruthyunjaya, T., and Ghosal, A., 2004. "A force-torque sensor based on a stewart platform in a near-singular configuration". *Mechanism and Machine Theory,* ***39***(9), pp. 971 – 998.

[20] Dwarakanath, T., Dasgupta, B., and Mruthyunjaya, T., 2001. "Design and development of a stewart platform based forcetorque sensor". *Mechatronics,* ***11***(7), pp. 793 – 809.

[21] Bhavikatti, S., Ranganath, R., and Ghosal, A., 2007. "A near-singular, flexure jointed, moment sensitive stewart platform based fore-torque sensor". In 13th National Conference on Mechanisms and Machines.

[22] Iliopoulos, A., Michopoulos, J., Orifici, A. C., and Thomson, R. S., 2011. "Experimental validation of the 2d meshless random grid method". In Proceedings of the ASME 2011 International Design Engineering Technical Conferences & Computers and Information in Engineering Conference IDETC/CIE, August 29-31, 2011, Washington, DC, USA. Submitted.

[23] Michopoulos, J., Hermanson, J. C., Iliopoulos, A., Lambrakos, S., and Furukawa, T., 2011. "Overview of constitutive response characterization for composite materials via data-driven design optimization". In Proceedings of the ASME 2011 International Design Engineering Technical Conferences & Computers and Information in Engineering Conference IDETC/CIE, August 29-31, 2011, Washington, DC, USA. Submitted.

[24] Michopoulos, J., Hermanson, J., Iliopoulos, A., Lambrakos, S., and Furukawa, T., 2011. "Data-driven design optimization for composite material characterization". *Journal of Computing and Information Science in Engineering,* ***11***(2). cited By (since 1996) 0.

[25] Gibson, W., 1962. "On the least-squares orthogonalization of an oblique transformation". *Psychometrika,* ***27***(2), pp. 193–195.

[26] Schonemann, P.. H., 1966. "A generalized solution of the orthogonal procrustes problem". *Psychometrika,* ***31***, p. 110.

[27] Higham, N. J., 2008. *Functions of Matrices: Theory and Computation*. Society for Industrial & Applied Mathematics,U.S., Mar.

[28] Levenberg, K., 1944. "A method for the solution of certain problems in least squares". *Quart. Applied Math.,* ***2***, pp. 164–168.

[29] Marquardt, D. W., 1963. "An algorithm for least-squares estimation of nonlinear parameters". *Journal of the Society for Industrial and Applied Mathematics,* ***11***(2), pp. pp. 431–441.

[30] Masroor, S. A., and Zachary, L. W., 1990. "Designing an all-purpose force transducer". In 1990 SEM Spring Conference on Experimental Mechanics, Vol. -1, pp. 327–330.

[31] Wickham, M. J., Riley, D. R., and Nachtsheim, C. J., 1995. "Integrating optimal experimental design into the design of a multi-axis load transducer". *Journal of engineering for industry,* ***117***(3), pp. 400–405.

[32] Doyle, J. F., 2004. "Inverse methods in experimental mechanics". In *Recent Advances in Experimental Mechanics*, E. E. Gdoutos, ed. Springer Netherlands, pp. 585–594.

[33] Meacham, E. M., and Doyle, J. F., 2007. "An inverse solution method for nonlinear problems using image data". *Measurement Science and Technology,* ***18***(9), Sept., pp. 2800–2808.

[34] Andrianopoulos, N. P., and Iliopoulos, A. P., 2005. *Strain measurements by a hybrid experimental-numerical method using a mesh-free field function, Honorary Volume for Professor P. S. Theocaris*. Armenian Academy of Sciences, pp. 31–41.

[35] Michopoulos, J. G., Hermanson, J. C., and Iliopoulos, A., 2010. "Towards a recursive hexapod for the multidimensional mechanical testing of composites". *ASME Conference Proceedings,* ***2010***(44113), pp. 91–99.

[36] Michopoulos, J., and Iliopoulos, A., 2011. "A computational workbench for remote full field 3d displacement and strain measurements". In Proceedings of the ASME 2011 International Design Engineering Technical Conferences & Computers and Information in Engineering Conference IDETC/CIE, August 29-31, 2011, Washington, DC, USA.